

## Bound-biexciton photoluminescence in CuCl thin films grown by vacuum deposition

This article has been downloaded from IOPscience. Please scroll down to see the full text article.

1999 J. Phys.: Condens. Matter 11 7653

(<http://iopscience.iop.org/0953-8984/11/39/320>)

View [the table of contents for this issue](#), or go to the [journal homepage](#) for more

Download details:

IP Address: 171.66.16.214

The article was downloaded on 15/05/2010 at 13:17

Please note that [terms and conditions apply](#).

## Bound-biexciton photoluminescence in CuCl thin films grown by vacuum deposition

M Nakayama, H Ichida and H Nishimura

Department of Applied Physics, Faculty of Engineering, Osaka City University, Sugimoto, Sumiyoshi-ku, Osaka 558-8585, Japan

Received 21 April 1999, in final form 22 June 1999

**Abstract.** We report on the photoluminescence properties of CuCl thin films with the thicknesses of 20 and 100 nm under intense-excitation conditions produced with a pulsed nitrogen laser. We have clearly observed two photoluminescence bands with a superlinear (almost quadratic) excitation-power dependence. The high-energy band is attributed to the well-known free-biexciton photoluminescence. The excitation-power dependence of the low-energy band exhibits a saturation behaviour when the free-biexciton band grows remarkably. In addition, the energy and shape of the low-energy band do not change with the excitation power, which is contrary to the characteristics of the free-biexciton photoluminescence reflecting the thermal distribution in the energy dispersion. From these facts, we conclude that the origin of the low-energy band is a bound biexciton. Furthermore, we find from the temperature dependence of the PL properties that the thermal dissociation of the bound exciton induces the instability of the bound biexciton.

### 1. Introduction

Cuprous halides such as CuCl and CuBr have attracted much attention for the past three decades in the field of excitonic properties of solids because the exciton binding energies (190 meV for CuCl and 108 meV for CuBr) are much larger than those for III–V and II–VI semiconductors [1, 2]. Such a large exciton binding energy leads to advantages as regards the observation of intense-excitation effects on excitons because of the high stability of the exciton. The formation of exciton molecules, so-called biexcitons, is a phenomenon typical of intense-excitation effects, and CuCl and CuBr crystals have proved model materials for the investigation of biexcitons. The binding energies of the biexcitons in CuCl and CuBr crystals are 34 and 25 meV, respectively [1]. These values are much larger than those for III–V and II–VI semiconductors. Although the optical gain mechanism due to biexcitons is a current topic of interest as regards quantum-well structures of wide-gap II–VI semiconductors [3, 4], this was first demonstrated in a CuCl bulk crystal a quarter-century ago [5]. Biexcitons bound to impurities, so-called bound biexcitons, have also been one of main subjects of interest as regards intense-excitation effects. In the early stage of the investigation of bound biexcitons, indirect-transition-type semiconductors such as GaP, Si, and Ge attracted considerable attention [6–8]. Recently, acceptor-bound biexcitons in II–VI CdSe, CdS, and ZnSe semiconductors were investigated by four-wave-mixing experiments [9–11]. It should be noted that there has been no experimental evidence found for the existence of bound biexcitons in cuprous halides. Hereafter, the well-known biexciton, which moves freely, will be called the free biexciton in analogy with the exciton.

In this paper, we report on the biexciton-related photoluminescence (PL) properties of CuCl thin films grown by vacuum deposition. In previous work [12], we demonstrated that crystalline thin films of CuCl and CuBr are easily prepared on (0001) Al<sub>2</sub>O<sub>3</sub> substrates by vacuum deposition in high vacuum, and discussed the hot-exciton properties of the thin films from the viewpoint of the exciton energy relaxation in momentum space. In the present work, we have focused on the intense-excitation effects on PL properties in CuCl thin films. Shuh *et al* [13] reported the observation of free-biexciton PL in CuCl thin films grown by molecular-beam epitaxy; however, they presented no discussion. We have clearly observed two PL bands with a superlinear (almost quadratic) excitation-power dependence. The high-energy band corresponds to the free-biexciton PL, while the low-energy band is attributed to the bound-biexciton PL whose intensity exhibits a saturation behaviour under the excitation condition of remarkable growth of the free-biexciton PL. We discuss the effects of the film thickness on the biexciton-related PL. Furthermore, we discuss the thermal stability of the bound biexciton on the basis of the temperature dependence of the PL properties.

## 2. Experimental procedure

The samples of CuCl thin films with layer thicknesses of 20 and 100 nm were grown on (0001) Al<sub>2</sub>O<sub>3</sub> substrates at 60 °C using a vacuum deposition method in high vacuum ( $\sim 1 \times 10^{-6}$  Torr). The substrates were heated to  $\sim 100$  °C in the vacuum chamber before the thin-film growth. Commercially supplied powders of CuCl with the purity of 99.9% were heated in a crucible, and the evaporation rate, which was controlled by monitoring the frequency of a crystal oscillator, was about 0.15 nm s<sup>-1</sup>. The evaporation rate was calibrated by measuring the thickness of some thin films with a profilometer. The uncertainty in the film thickness is estimated to be around 10%. From the measurements of the x-ray diffraction patterns, we confirmed that crystalline thin films were grown preferentially along the  $\langle 111 \rangle$  direction [12].

In the PL measurements under intense-excitation conditions, the excitation source was a pulsed nitrogen laser with the pulse width of  $\sim 300$  ps and the maximum pulse power of  $\sim 30$   $\mu$ J. A He–Cd laser with a 325 nm line was used for measuring weak-excitation PL spectra: the excitation power was  $\sim 0.1$  W cm<sup>-2</sup>. Photoluminescence spectra were analysed using a multi-channel detection system attached to a 32 cm single monochromator with a resolution of 0.5 nm. Absorption spectra were measured with a double-beam spectrometer with a resolution of 0.2 nm. The sample temperature was controlled using a closed-cycle helium-gas cryostat.

## 3. Results and discussion

Before describing the biexciton-related PL properties of CuCl thin films, we show the PL spectra of the 100 nm and 20 nm CuCl thin films under a weak-excitation condition and the absorption spectrum of the 20 nm film at 10 K in figure 1 for the assignment of the fundamental excitons. In a CuCl crystal, the top of the valence band is the split-off hole ( $\Gamma_7$ ), which is  $\sim 60$  meV away from the degenerate heavy-hole and light-hole ( $\Gamma_8$ ) bands. This valence-band structure is in the reverse order to that in ordinary semiconductors. The exciton consisting of the  $\Gamma_7$  ( $\Gamma_8$ ) hole and  $\Gamma_6$  electron has been historically called the  $Z_3$  ( $Z_{1,2}$ ) exciton. In figure 1, the energy of the PL band labelled  $Z_3$  exactly agrees with that of the  $Z_3$ -exciton absorption band, so the PL band is due to the free-exciton emission. The low-energy PL band is attributed to the emission from an exciton bound to an impurity which has been called the  $I_1$  bound exciton. The type of the impurity has been assigned as a neutral acceptor: a possible candidate is a Cu<sup>+</sup> vacancy [14]. The observed energies of the  $Z_3$  free exciton and  $I_1$  bound exciton

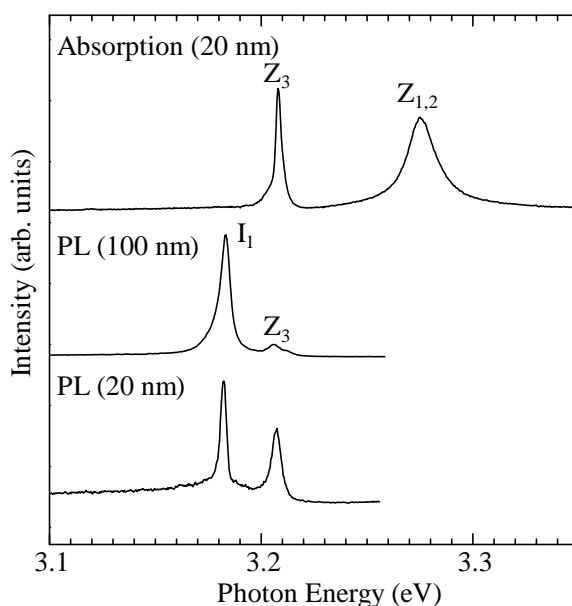


**Figure 1.** Photoluminescence spectra of the 100 nm and 20 nm CuCl thin films under a weak-excitation condition and the absorption spectrum of the 20 nm film at 10 K.

almost agree with those in a CuCl bulk crystal, 3.203 and 3.181 eV at 8 K, respectively [15]. The slight discrepancy might be due to the thermal strain in the thin film. It is noted that the quantum-size effect on the free exciton is negligible even for the 20 nm film because the Bohr radius is about 0.7 nm. In a bulk crystal, a broad PL band due to impurities is usually observed on the low-energy side of the  $I_1$  band [15]; however, it does not appear in the thin films as shown in figure 1. This is an advantage as regards observing the biexciton-related PL because its energy range overlaps with that of the broad PL band.

Figure 2 shows the PL spectra of the 100 nm CuCl thin film under various excitation conditions at 10 K, where every spectrum under the intense-excitation condition with the pulsed nitrogen laser is scaled by the given factor. From figure 2, it is obvious that there are two PL bands peculiar to the intense-excitation conditions. One is the PL band labelled  $N_1$  which appears at 3.149 eV. Its energy almost agrees with that of the so-called  $N_1$  band (3.145 eV at 8 K) which was observed with the free-biexciton PL in a CuCl bulk crystal [16]. We note that its origin has not been revealed until now. The other is the PL band labelled M in the energy range between the  $N_1$  and  $I_1$  bound-exciton bands. The energy of the M-PL band coincides with that of the well-known free-biexciton PL. In a bulk crystal, it is known that there exist two types of free-biexciton PL,  $M_T$  and  $M_L$  [1]: the  $M_T$  ( $M_L$ ) band corresponds to the emission from the free biexciton to the transverse (longitudinal) exciton. The reported energies of the  $M_T$  and  $M_L$  bands are 3.171 and 3.165 eV at 1.6 K, respectively [17]. In the present PL spectra of the thin film, we cannot resolve the two types of free-biexciton bands because of the broad shape. We note that the two PL bands could not be separated with a higher resolution of 0.2 nm. The broad PL shape may be due to the inhomogeneous broadening and/or high effective temperature. As the excitation power increases, the peak energy of the free-biexciton-PL band shifts to the low-energy side, and the line shape becomes broader. These characteristics reflect the thermal distribution of the free biexcitons in the dispersion relation in momentum space. On the other hand, the energy and shape of the  $N_1$ -PL band do not

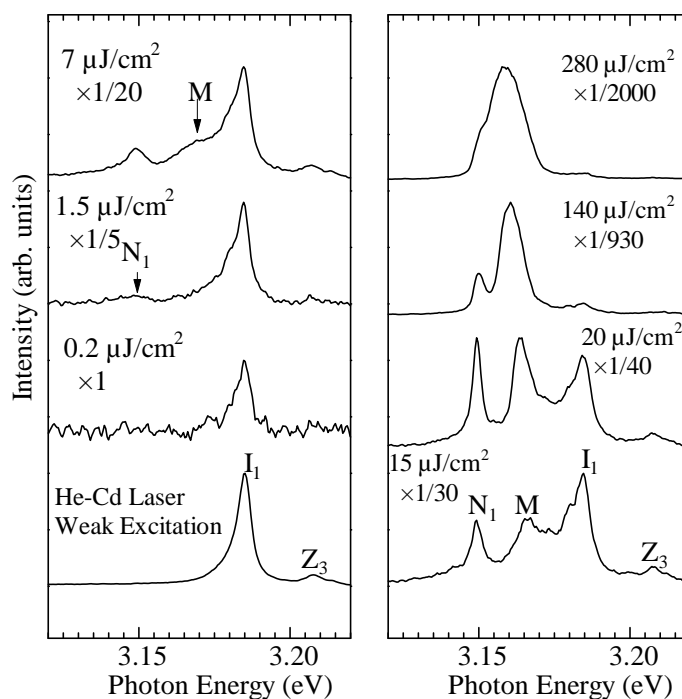
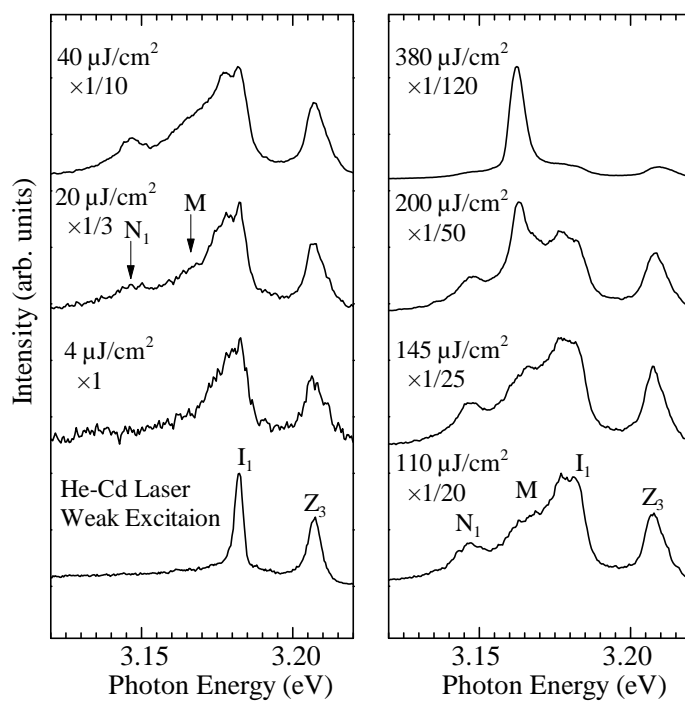


**Figure 2.** Photoluminescence spectra of the 100 nm CuCl thin film under various excitation conditions at 10 K, where every spectrum under the intense-excitation condition with the pulsed nitrogen laser is scaled by the given factor.

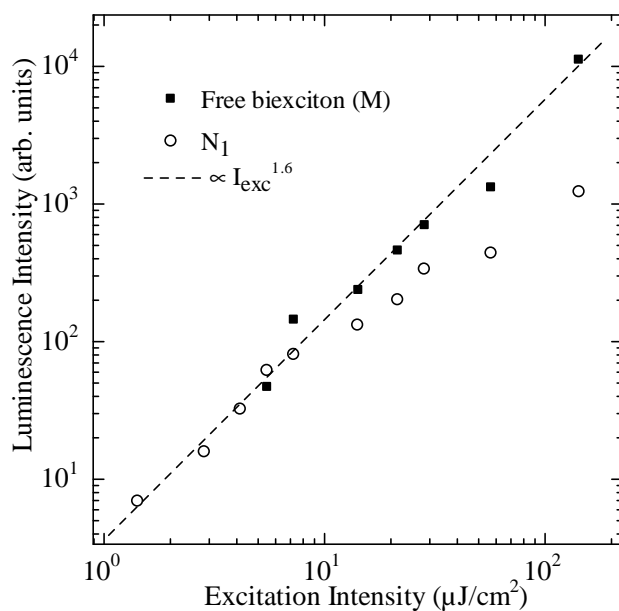
change with the excitation power. Moreover, it is noted that its intensity exhibits a saturation behaviour relative to that of the free-biexciton-PL band. These features of the  $N_1$ -PL band suggest that it originates from a state bound to an impurity.

Figure 3 shows the PL spectra of the 20 nm CuCl thin film under various excitation conditions at 10 K, where every spectrum excited by the pulsed nitrogen laser is scaled by the given factor. We observe the  $N_1$  and free-biexciton (M) bands, which are described above in connection with figure 2, under the intense-excitation conditions. In the 20 nm film, an additional PL band remarkably appears on the low-energy side of the  $I_1$  bound-exciton band. This PL band, which also appears as the shoulder of the  $I_1$  band in the 100 nm film (figure 2), is assigned to the emission of the  $Z_3$  exciton assisted by one longitudinal optical (LO) phonon because the energy difference from the  $Z_3$  exciton coincides with the LO-phonon energy (26 meV) [1]. Thus, the free-biexciton-PL and  $N_1$ -PL bands are commonly observed in CuCl thin films. We note that the appearance of the two PL bands in the 20 nm film needs higher excitation power, compared with that in the 100 nm film, which will be discussed later.

We focus on the excitation-power dependence of the integrated intensities of the  $N_1$ -PL and free-biexciton-PL bands in the 100 nm film, which is depicted in figure 4. In the decomposition of every PL band, a Gaussian line-shape function was applied. Although it is well known that the line shape of the free-biexciton band is an inverse Boltzmann type producing an asymmetric shape with a low-energy tail, the observed shape is almost symmetric as shown in figures 2 and 3. This seems to be due to the fact that the broad line shape hides the asymmetry. The errors in the Gaussian fitting are around 10%. It is evident from figure 4 that the intensity of the free-biexciton PL ( $I_M$ ) exhibits a typical superlinear dependence of the



**Figure 3.** Photoluminescence spectra of the 20 nm CuCl thin film under various excitation conditions at 10 K, where every spectrum under the intense-excitation condition with the pulsed nitrogen laser is scaled by the given factor.



**Figure 4.** Excitation-power dependence of the integrated intensities of the  $N_1$ -PL and free-biexciton- (M-) PL bands at 10 K in the 100 nm CuCl film.

excitation power ( $I_{\text{exc}}$ ):  $I_M \propto I_{\text{exc}}^{1.6}$ . The excitation-power dependence of the  $N_1$ -PL intensity ( $I_{N_1}$ ) has the following two characteristics: (i) the superlinear dependence like that of the free biexciton,  $I_{N_1} \propto I_{\text{exc}}^{1.6}$ , before the remarkable growth of the biexciton-PL band; and (ii) the saturation behaviour after that. The former and latter indicate that the  $N_1$ -PL band has a biexciton nature and that it is related to a state bound to an impurity, respectively. As discussed above in connection with figure 2, the fact that the energy of the  $N_1$ -PL band does not depend on the excitation power also suggests the impurity origin. These findings lead to the conclusion that the  $N_1$ -PL band originates from a bound biexciton. The likeliest candidate for the impurity is considered to be the neutral acceptor, just like the case for the  $I_1$  bound exciton, because another impurity-related PL is not observed under weak-excitation conditions. In addition, it is obvious that the  $I_1$ -PL intensity shown in figure 2 decreases remarkably in the excitation-power region above  $15 \mu\text{J cm}^{-2}$ , where the  $N_1$ -PL intensity exhibits saturation behaviour as shown in figure 4. This also suggests that the impurities related to the  $I_1$ - and  $N_1$ -PL bands are identical. Hereafter, we will call the  $N_1$ -PL band the bound-biexciton PL.

Next, we discuss the binding energy of the bound biexciton. It is considered that the bound-biexciton PL results from the optical transition from the bound-biexciton state,  $(A^0, M)$ , to the  $I_1$  bound-exciton state,  $(A^0, X)$ , where the free biexciton,  $Z_3$  free exciton, and neutral acceptor are denoted by M, X, and  $A^0$ , respectively. Figure 5 shows the energy schemes of the free states on the right-hand side and the bound states on the left-hand side. The energies of the states labelled X and M correspond to the lowest energies of the dispersion relations of the  $Z_3$  free exciton and free biexciton, respectively. According to the energy schemes, we can straightforwardly estimate the binding energy of the bound biexciton ( $E_{b, \text{BM}}$ ) from the observed PL energies. Here, we use the PL energies in the 100 nm film. Although the estimation of the energy of the M state needs a line-shape analysis of the free-biexciton-PL band based on the well-known inverse Boltzmann distribution function, the analysis is not effective in the present case because the line shape is broad and almost symmetric as described above in the discussion of figure 4. Using the reported biexciton binding energy ( $E_{b, \text{M}}$ ) of 34 meV and the observed  $Z_3$  free-exciton energy of  $3.207 \pm 0.001$  eV, the energy spacing between the M and X states in figure 5 is estimated to be  $3.173 \pm 0.001$  eV. This energy agrees with the high-energy

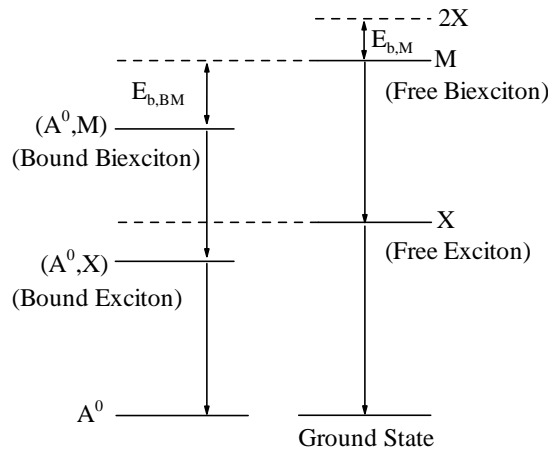


**Figure 5.** Energy schemes of the free states (right-hand side) and the bound states (left-hand side), where the free biexciton,  $Z_3$  free exciton, and neutral acceptor are denoted by M, X, and  $A^0$ , respectively. The binding energies of the free and bound biexcitons are denoted by  $E_{b, \text{M}}$  and  $E_{b, \text{BM}}$ , respectively.

edge of the free-biexciton-PL band which is obvious in the PL spectra at 140 and 280  $\mu\text{J cm}^{-2}$  shown in figure 2. This fact is consistent with the characteristics of the line shape of the free-biexciton-PL band. The energies of other PL bands correspond to the peak energies whose errors are around 1 meV. Consequently, the binding energy of the bound biexciton is estimated to be  $46 \pm 2$  meV. In II–V semiconductors, the binding energies of the bound biexcitons related to neutral acceptors in ZnSe and CdS are 10 and 18 meV, respectively [11]. It is noted that the above energies of the II–VI semiconductors are corrected for the difference in definition of the binding energy because the binding energy listed in reference [11] is measured from twice the free-exciton energy. The binding energies of the free biexcitons of ZnSe, CdS, and CuCl are 3.5 [11], 6.3 [11], and 34 meV, respectively. Thus, the order of the binding energies of the bound biexcitons is consistent with that of the free biexcitons. To our knowledge, there has been no report on theoretical studies of the binding energies of the bound biexcitons, so quantitative discussion is beyond the scope of the present paper.

Here, we discuss the difference between the PL properties of the films that are 100 nm and 20 nm thick. From the PL spectra in figures 2 and 3, it is obvious that the appearance of the free-biexciton and bound-biexciton bands in the 20 nm films needs much higher excitation power, compared with that in the 100 nm film: the bound-biexciton- ( $N_1$ -) PL band appears at 1.5  $\mu\text{J cm}^{-2}$  in the 100 nm film, while no biexciton-related band appears at 4  $\mu\text{J cm}^{-2}$  in the 20 nm film. The excitation power for the appearance of the biexciton-related PL bands in the 20 nm film is about one order higher than that in the 100 nm film. It is noted that the appearance of the PL bands is not related to the existence of an excitation threshold but to the sensitivity of the detection system. In order to explain the above PL properties, we focus on the PL intensities of the  $Z_3$  free exciton and  $I_1$  bound exciton under the weak-excitation condition. From figure 1, it is obvious that the relative PL intensity of the  $Z_3$  free exciton with respect to the  $I_1$  bound exciton in the 20 nm film is much stronger than that with respect to the one in the 100 nm film. Under weak-excitation conditions, it was already confirmed that the relative PL intensity of the  $Z_3$  band with respect to the  $I_1$  one increases as the film thickness decreases, and the following explanation was proposed [12, 13]. In thin films, it is expected that ballistic collisions of the free excitons with the film boundaries, so-called wall collisions, occur frequently. On the other hand, the bound exciton should be insensitive to the film thickness because of the localization nature. Assuming that the wall collisions open a new radiative decay channel, which shortens the radiative lifetime of the free exciton, the above film-thickness dependence of the relative PL intensity is understandable because the radiative efficiency of the free exciton increases with the decrease of the film thickness. The radiative lifetime of the  $Z_3$  free exciton in the 20 nm film is estimated to be of the order of picoseconds [13]. Since the biexcitons are formed by exciton–exciton collisions, it is considered that the shorter free-exciton lifetime in a thinner film results in the lower efficiency of the biexciton formation. This seems to be a major reason for the excitation-power difference as regards the appearance of the biexciton-related PL bands in the 20 and 100 nm films. From the scenario of the above wall-collision model, it is also expected that the bound-biexciton PL in the 20 nm film is relatively suppressed in comparison with that in the 100 nm film, similarly to the case of the  $I_1$  bound exciton. In the PL spectra of the 100 nm film (figure 2), with increasing excitation power, the bound-biexciton band appears first, then the free-biexciton band appears. On the other hand, in the 20 nm film (figure 3), the two PL bands simultaneously appear, then the bound-biexciton band does not grow remarkably. Thus, the film-thickness dependence of the biexciton-related PL is qualitatively explained in the framework of the wall-collision model.

Finally, we discuss the PL properties of the bound biexciton from the viewpoint of the thermal stability. Figure 6 shows the PL spectra of the 100 nm CuCl thin film under weak- and intense-excitation conditions, which are depicted on the left-hand and right-hand sides,



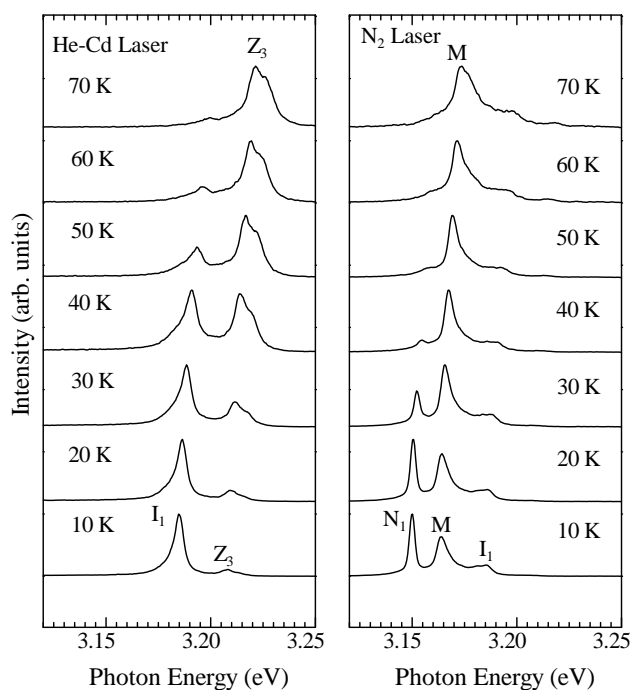


**Figure 6.** Photoluminescence spectra of the 100 nm CuCl thin film under weak- and intense-excitation conditions, which are depicted on the left- and right-hand sides, respectively, at various temperatures.

respectively, at various temperatures. It is obvious that the PL intensities of the bound exciton ( $I_1$ ) and bound biexciton ( $N_1$ ) decrease with reference to those of the free exciton ( $Z_3$ ) and free biexciton ( $M$ ) as temperature increases. This temperature dependence can be considered to be due to the thermal dissociation of the bound states. Figure 7 shows the intensity ratio of the  $I_1$  bound-exciton PL to the  $Z_3$  free-exciton PL,  $I_{I_1}/I_{Z_3}$ , and that of the bound-biexciton PL to the free-biexciton PL,  $I_{N_1}/I_M$ , as a function of inverse temperature ( $1/T$ ). From the linear slope in the high-temperature region in figure 7, we can estimate the thermal activation energies of the bound exciton and bound biexciton. It is noted that the slope of the bound biexciton agrees with that of the bound exciton. Similar results have been obtained for the 20 nm film. The estimated value of the thermal activation energy is  $20 \pm 4$  meV. Although the value contains a large error, which is due to the narrow region of the linear slope shown in figure 7, it is almost consistent with the binding energy of the bound exciton, 22 meV, obtained from the energy difference between the free-exciton-PL and bound-exciton-PL bands. This is reasonable for the bound exciton. On the other hand, the thermal activation energy is about half of the binding energy of the bound biexciton (46 meV). This fact suggests that the thermal dissociation of the bound exciton, which is the core of the bound biexciton, induces the instability of the bound biexciton.

#### 4. Conclusions

We have observed two PL bands under intense-excitation conditions in CuCl thin films with the thicknesses of 20 and 100 nm. The high-energy PL band is attributed to the well-known

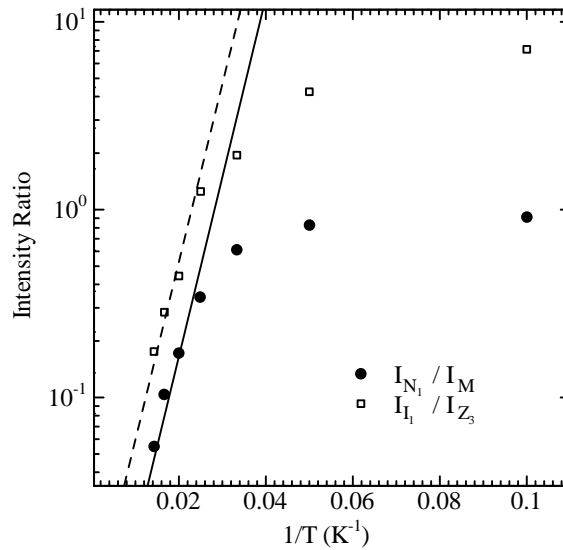


**Figure 7.** The intensity ratio of the  $I_1$  bound-exciton PL to the  $Z_3$  free-exciton PL,  $I_{I_1}/I_{Z_3}$ , and that of the bound-biexciton PL to the free-biexciton PL,  $I_{N_1}/I_M$ , as a function of inverse temperature ( $1/T$ ).

free biexciton. The excitation-power dependence of the intensity of the low-energy PL band exhibits a superlinear dependence (almost quadratic) similar to that of the free biexciton; however, it reveals a saturation behaviour after the remarkable growth of the free-biexciton band. Furthermore, the energy and shape of the low-energy band do not change with the excitation power, which is contrary to the characteristics of the free biexciton reflecting the distribution in the energy dispersion. These facts indicate that the origin of the low-energy PL band is a biexciton bound to an impurity, a bound biexciton. The impurity of the bound biexciton is considered to be the same as that of the  $I_1$  bound exciton, a neutral acceptor, because we observe nothing else for impurity-related PL bands under weak-excitation conditions. The binding energy of the bound biexciton is estimated to be  $46 \pm 2$  meV. The PL properties of the free and bound biexcitons depend on the film thickness: in the thinner film, the formation of total biexcitons is suppressed, and the relative intensity of the bound-biexciton PL and the free-biexciton PL is decreased. This is qualitatively explained in the framework of the wall-collision model of the free excitons and biexcitons, assuming that their collisions with the film boundaries open new radiative decay channels and shorten the lifetimes. In addition, we find from the temperature dependence of the PL spectra that the thermal stability of the bound biexciton is similar to that of the bound exciton. The thermal activation energy of the bound biexciton is equal to that of the bound exciton, and it agrees with the binding energy of the bound exciton. This suggests that the thermal dissociation of the bound exciton which is the core of the bound biexciton induces the instability of the bound biexciton.

## References

- [1] For a review, see Ueta M, Kanzaki H, Kobayashi K, Toyosawa Y and Hanamura E 1986 *Excitonic Processes in Solids* (Berlin: Springer) ch 2, p 20 for biexcitons and ch 3, p 116 for cuprous halides
- [2] For a review, see Hönerlage G, Lévy R, Grun J B, Klingshirn C and Bohnert K 1985 *Phys. Rep.* **124** 161
- [3] Kreller F, Lowisch M, Plus J and Henneberger F 1995 *Phys. Rev. Lett.* **75** 2420

- [4] Kozlov V, Kelkar P, Vertikov A, Nurmikko A V, Chu C-C, Han J, Hua C G and Gunshor R L 1996 *Phys. Rev. B* **54** 13932
- [5] Shaklee K L, Leheny R F and Nahory R E 1971 *Phys. Rev. Lett.* **26** 888
- [6] Merz J L, Faulkner R A and Dean P J 1969 *Phys. Rev.* **188** 1228
- [7] Sauer R 1973 *Phys. Rev. Lett.* **31** 376
- [8] Martin R W 1974 *Solid State Commun.* **14** 369
- [9] Erland J, Razbirin B S, Lyssenko V G, Pantke K-H and Hvam J M 1994 *J. Cryst. Growth* **138** 800
- [10] Razbirin B S, Nel'son D K, Erland J, Pantke K-H, Lyssenko V G and Hvam J M 1995 *Solid State Commun.* **93** 65
- [11] Kutzer V, Lummer B, Heitz R, Hoffmann A, Broser I, Kurtz E and Hommel D 1996 *J. Cryst. Growth* **159** 776
- [12] Nakayama M, Soumura A, Hamasaki K, Takeuchi H and Nishimura H 1997 *Phys. Rev. B* **55** 10099
- [13] Shuh D K, Williams R S, Segawa Y, Kusano J, Aoyagi Y and Namba S 1991 *Phys. Rev. B* **44** 5827
- [14] Certier M, Wecker C and Nikitine S 1969 *J. Phys. Chem. Solids* **30** 2135
- [15] Goto T, Takahashi T and Ueta M 1968 *J. Phys. Soc. Japan* **24** 314
- [16] Souma H, Goto T, Ohta T and Ueta M 1970 *J. Phys. Soc. Japan* **29** 697
- [17] Nagasawa N, Nakata N, Doi Y and Ueta M 1975 *J. Phys. Soc. Japan* **39** 987